Hydrophobic Noncovalent Interactions of Inosine–Phenylalanine: A Theoretical Model for Investigating the Molecular Recognition of Nucleobases

ARTICLE *in* THE JOURNAL OF PHYSICAL CHEMISTRY A · MAY 2014

Impact Factor: 2.69 · DOI: 10.1021/jp411230w

4 AUTHORS, INCLUDING:

Lucas De Azevedo Santos
Universidade Federal de Lavras (UFLA)
4 PUBLICATIONS **18** CITATIONS
SEE PROFILE

Matheus Freitas
Universidade Federal de Lavras (UFLA)
111 PUBLICATIONS **1,158** CITATIONS
SEE PROFILE

Teodorico C. Ramalho
Universidade Federal de Lavras (UFLA)
188 PUBLICATIONS **1,685** CITATIONS
SEE PROFILE

THE JOURNAL OF PHYSICAL CHEMISTRY A

Article

pubs.acs.org/JPCA

Hydrophobic Noncovalent Interactions of Inosine-Phenylalanine: A Theoretical Model for Investigating the Molecular Recognition of Nucleobases

Lucas A. Santos, Elaine F. F. da Cunha, Matheus P. Freitas, and Teodorico C. Ramalho*

Department of Chemistry, Federal University of Lavras, CEP 37200-000 Lavras, Minas Gerais Brazil

Supporting Information

ABSTRACT: Understanding the molecular recognition process of nucleobases is one of the greatest challenges for both computational chemistry and biophysics fields. In fact, our results point out that it is a hard task to take into account the hydrophobic interactions, such as $\pi-\pi$ and T-stacking interactions, by theoretical calculations using conventional force fields due to quantum effects of hyperconjugation and electronic correlation. In this line, our findings put in evidence that simple modifications in the Lennard-Jones potential can improve theoretical predictions in scenarios where hydrophobic interactions can drive the molecular recognition.

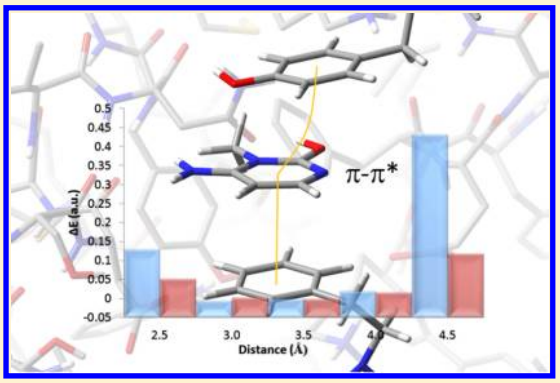

1. INTRODUCTION

Currently, the understanding of biological processes, such as molecular recognition or folding protein, is one of the greatest challenges for both computational chemistry and physical chemistry.[1] For instance, the molecular recognition in biological systems relies on the existence of specific attractive interactions between two partner molecules. Recently, Ben-Naim reported that solvent effects and electrostatic forces are important factors responsible for the folding process in proteins, activating this discussion.[2,3] Nevertheless, some other findings reinforce that hydrophobic interactions can play a significant role in driving the molecular recognition process in biological systems.[4,5] Despite the basic principles of the hydrophobic and noncovalent interactions being well-established, just recently theoretical models have been able to explain and quantify many features of this important phenomenon, which can have its origin in electronic effects.[6]

In fact, aromatic amino acids or nucleosides act as a relevant class in biochemistry, which can lead to noncovalent interactions.[7,8] In this case, inosine can be considered a model molecule because it is commonly found in tRNAs and is essential for proper translation of the genetic code. It is also important to mention that the role of nonbonded interactions in peptide conformation deserves special attention, and the study in amino acids is expected to give insights to support structural assumptions necessary to interpret some molecular biology phenomena. In this line, phenylalanine (Phe) is often chosen as a representative unit of the hydrophobic backbone in a protein in order to simulate possible interactions in biology, where the hydrophobic interactions can take place. Indeed, amino acids can perform some specific hydrophobic interactions, which involve high electronic correlation, namely $\pi-\pi^*$ stacking and T-stacking interactions.[9−11] They are the key to understanding and controlling a variety of phenomena, such as DNA interactions, the packing structure of aromatic molecules, and interactions between biological compounds and the enzyme receptors, and they are present in a wide variety of compounds, having interesting reactivity and physical properties.[12−14] These systems have notorious sensitivity and depend heavily on the surrounding components. In fact, a convenient substituent in the aromatic structure can generate significant electronic effects over the energy and structure of a given system.[15−17]

Notwithstanding, relevant findings revealed an interesting property of that kind of interaction when occurred between aromatic amino acids. Once they are at neutral state, the discrete water solvent does not affect the power of $\pi-\pi^*$ and T-shaped interactions.[18] Accordingly, methods with high accuracy are crucially required, so that they can be used accurately to obtain all electronic effects.[19−21] The most ordinary and suitable methods are Møller−Plesset (MP) perturbation theory, density functional theory (DFT), or DFT-D (density functional theory with dispersion correction) with an appropriate basis set.[7,17,22−26]

It is well-known that the Kohn−Sham DFT is a leading method for electronic structure calculations in chemistry,

Special Issue: Energetics and Dynamics of Molecules, Solids, and Surfaces - QUITEL 2012

Received: November 15, 2013
Revised: May 6, 2014
Published: May 9, 2014

mainly because of its high efficiency and relatively low computational cost. Nevertheless, despite the recent improvements in DFT, there are still difficulties in using DFT to properly describe intermolecular interactions, especially van der Waals forces (dispersion) and charge transfer excitations due to the lack of exact Hartree−Fock exchange in some functionals.[27−30] In this line, some density functionals, such as B97-D, have been demonstrated to be efficient in describing $\pi-\pi^*$ interactions with satisfactory agreement with SCS-MP2, which is a powerful method developed in order to overcome this problem.[17,20,31,32]

Nevertheless, a critical fact for large biological systems is that highly correlated ab initio methods are also highly computationally demanding. Molecular mechanics methods try to overcome this problem in a simple way. Molecular mechanics-based methods involving docking studies and also molecular dynamics simulations using force fields are suitable tools to adjust ligands at target sites and to estimate interaction energy (affinity) and to evaluate protein folding.[33] Currently, this is a well-established technique applied to numerous cases.[34−36]

It should be kept in mind, however, that a delicate point in the MM technique is related to the use of corrected potential and parameters for force fields. Recently, Rappé and co-workers developed a universal force field able to describe organic and inorganic elements for molecular mechanics and molecular dynamics simulations called UFF.[37] The UFF equation can be described by eq 1:

$$E = E_R + E_\theta + E_\varnothing + E_\omega + E_{el} + E_{vdw} \quad (1)$$

This equation defines the potential energy of the system whose first term, E_R, describes the bond stretching. Two possible ways to describe the bond stretch interaction (E_R) have been described: as a harmonic oscillator or as the Morse function. The angular distortions are expressed by E_θ (bond angle bending), $E_\varnothing$ (dihedral angle torsion), and E_ω (inversion terms). The electrostatic interactions are included by E_{el}. Both E_{el} and E_{vdw} represent the nonbonded terms in force fields. However, the crucial term of this line is the last one, which applies the hydrophobic nonbonded energy. In other words, it describes the van der Waals forces from the intramolecular interactions. For investigating hydrophobic nonbonded interactions, the Lennard-Jones (LJ) potential[38,39] has been used on most of the force fields.

$$E_{vdw} = \varepsilon\left\{\left(\frac{r_e}{r}\right)^{12} - 2\left(\frac{r_e}{r}\right)^{6}\right\} \quad (2)$$

The parameter ε represents the energy depth, and r_e is the equilibrium distance of the interaction.[37,40]

A previous work[5] has taken into account the ability of MM techniques to describe energy interactions among amino acids comparing the MM results to high electronic correlation methods. In this case, the larger difference lies when the repulsive energies prevail, more precisely, closer to equilibrium distance. Interestingly, in this case the relative energy values between MP2 and UFF can be quite different. To elucidate this fact, the repulsive forces will be taken as the main question.

In line with this, the goal of this work is to evaluate the relevance of the noncovalent effects for dimeric structures of phenylalanine and inosine, which represent a very important model for understanding hydrophobic interactions. Our work calls attention to the nonbonded energies, trying to propose new correction terms in familiar potentials to approach them to the results obtained by efficient quantum methods.

2. METHODOLOGY

2.1. Computational Methods. In the first stage, the computational calculations were performed separately for each monomer (Figure 1). The theoretical calculations were

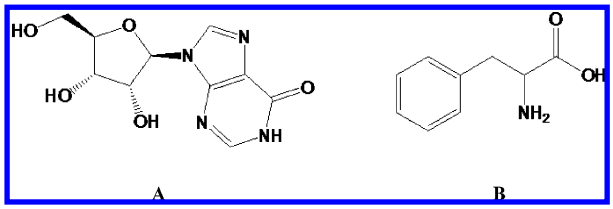

Figure 1. Studied monomer structures: (A) inosine and (B) phenylalanine.

performed using Gaussian09,[41] and the optimizations were carried out at the B3LYP/6-31+G** calculation level. The absolute minimum point was obtained by carrying out a conformational search using the Monte Carlo method with Spartan Pro.[42]

After that, the dimers (Figure 2) were built following four known possible conformations:[9,16,17] parallel eclipsed (PE), parallel staggered (PS), parallel displaced (PD), and T-Shaped (TS). The Angular (Ang) conformation was proposed in this work, in order to evaluate an intermediate geometry between the parallel and T conformations. The potential energy curve was plotted for each conformation by single point calculations through the UFF method. The farther point of the interaction was fixed at 8.0 Å. With the same idea, single point and NBOdel calculations[43] were performed at the DFT level using several functional and basis set, in order to obtain the hyperconjugation energies to understand the nonbonded interaction effects.

2.2. Potential Function Formulation. Potential energy curves (PEC) were plotted following the Lennard-Jones potential and compared to the Møller−Plesset perturbation theory results, which were taken as a reference. The basis set superposition error (BSSE) for the dimeric structures was estimated using the counterpoise correction method.

3. RESULTS AND DISCUSSION

3.1. Hyperconjugation Analysis. The interaction energy (ΔE) between A and B was calculated using eq 3:

$$\Delta E_{(r)} = E^{AB}_{(r)} - (E^A + E^B) \quad (3)$$

where E^A and E^B are the energies of the isolated objects (monomers) and E^{AB} the energy of their interacting assembly (dimer).

Initially, in order to evaluate the interaction energy between inosine and phenylalanine molecules, we have used electronic structure methods for taking into account the electronic effects, such as hyperconjugative interactions.

To reach the understanding of hyperconjugative effects in the interaction models (Figure 2), the NBOdel calculations were carried out (Figures 3 and 4). However, to ensure that our findings are reliable, the DFT values have been compared to the MP2 as well as DFT-D results using the GTO and CBS basis set (Figure 3). In order to evaluate the electronic effect for hydrophobic interaction, we have constructed potential energy

dx.doi.org/10.1021/jp411230w | J. Phys. Chem. A 2014, 118, 5808−5817

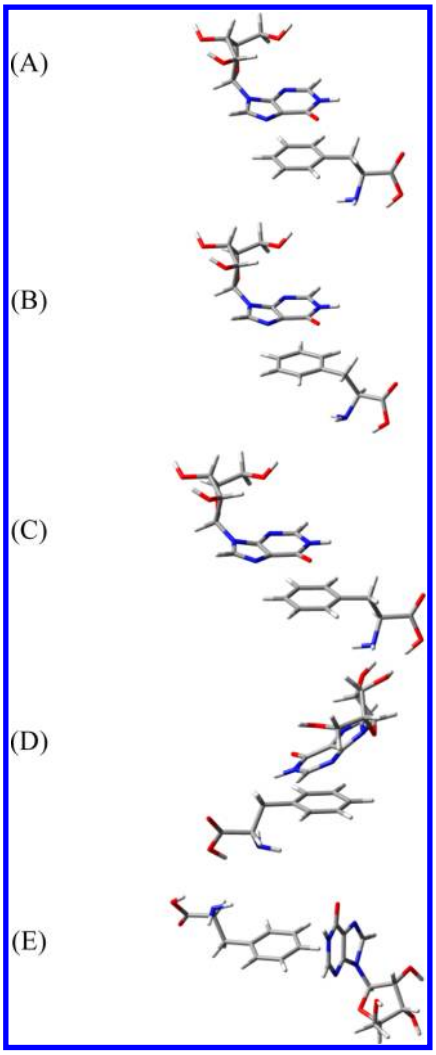

Figure 2. Dimer's geometry configuration: (A) parallel eclipsed, (B) parallel staggered, (C) parallel displaced, (D) angular, and (E) T-shaped. Carbon in gray, nitrogen in blue, oxygen in red, and hydrogen in white.

curves (PEC) for the model systems, which could simulate noncovalent interactions involved in the molecular recognition process. Actually, the concept of the PEC plays a critical role in the understanding of chemical reactions as well as description, simulation, and modeling of molecular systems.[7]

It is certainly worth noticing that the NBOdel results (Figures 3 and 4) give three energy types: the energy of deletion (E_{Lewis}), the total energy (E_{total}), and the energy change (E_{hyp}). The last one can be obtained by subtracting the total energy from the energy of deletion (eq 4).

$$\Delta E_{hyp} = \Delta E_{Lewis} - \Delta E_{total} \quad (4)$$

The PECs in Figure 3 show the ability of different methods to deal with the proposed situation for PE and TS conformations (the full data can be found in Figures S3−S5 of the Supporting Information). By looking at ΔE_{total}, our findings indicate that all the PECs have the same trend, except for MP2/cc-pvdz, which pointed the PE's r_e at 3.0 Å when actually it is at 3.5 Å. So, it cannot be used as an appropriate reference benchmark to these systems. In fact, more accurate energy values for hydrophobic interactions can be obtained with DFT-D methods. It is known that popular density functionals cannot describe correctly van der Waals interactions resulting from dynamical correlations between fluctuating charge distributions. Thus, a pragmatic method to overcome this problem has been given by Grimme and coworkes.[44,45] The ΔE_{hyp} PECs have shown higher values with the functional M062X-D3. A similar fact occurs to B97-D/cc-pvdz and B97-D3/cc-pvdz as well.

In accordance with Table 1, the lower energy values can be obtained, in general, with the B97-D3 and B97-D functional with the 6-31+G** basis set. In this system, MP2/6-31+G** seems to be a satisfactory method as well, producing lower energies at low-range interactions (Figure 3). In general, the functional M062X-D3 has shown the highest values among the four DFT methods tested.

Although it is possible to detect small differences among MP2, B97-D, and B97-D3, their trends are the same in relation to the energy minima, r_e, and also the repulsive forces. The opposite occurs when the UFF and MP2 results were analyzed.[5] Between the basis sets tested, the choice of the basis set 6-31+G** improved the results according to our proposal. Besides the 6-31+G** basis set has been shown to be satisfactory on similar structures.[11,26,46]

In a previous publication,[5] we noticed high discrepancies in relative interaction energy (ΔE) between UFF and MP2 methods, when the dimeric structures get closer beyond the most stable configuration (Figure S1 of the Supporting Information). It should be kept in mind, however, that a proper understanding of this phenomenon requires a deeper evaluation of both electronic and steric effects involved in the molecular interaction. Therefore, more information can be extracted by looking into the splitting behavior of Figure 4.

The ΔE_{hyp} value obtained from eq 4 is the contribution of the antibonding orbitals through hyperconjugative effects all over the interaction. By using eq 4, it is possible to extract ΔE_{total} from the DFT results reported in Figure 3 and Figure S3 of the Supporting Information. In this context, the variance of the orange and the blue bars will be the ΔE_{total} of the system (Figure 4). The ΔE_{total} will be positive if $|\Delta E_{Lewis}|$ is higher. A negative signal will appear if $|\Delta E_{hyp}|$ is higher. Accordingly, high ΔE_{hyp} values will act synergistically to stabilize the interaction. Lower ΔE_{hyp} values should be interpreted as an orbital repulsion, and it will destabilize the system, giving high ΔE_{total} values.

It is noteworthy that, in Figure 4, the blue and orange bars show an energy minimum point at 4.0 Å for PE and PS, while 2.5 and 3.5 Å are observed for PD and Ang conformations, respectively. Surprisingly, the energy minima will move to 3.5, 3.5, and 3.0 Å, respectively, if the values of blue and orange bars are summed (Figure 3 and Figure S3 of the Supporting Information).

By looking at the ΔE_{total} values for PE, PS and Ang, it is possible to notice that r_e has been decreased due to the hyperconjugative effects, and, in a distinct way, r_e has been increased for PD and TS. In TS, the ΔE_{Lewis} and ΔE_{hyp} do not act synergistically, these findings suggest a simple electrostatic interaction due to a plausible polarization. The distance between ring hydrogen of inosine and nearest atom of the phenylalanine is 2.8 Å. ΔE_{Lewis} has an energy minimum at 1.0 Å. Furthermore, even at the very close distance of 0.5 Å, the ΔE_{hyp} is negative, contributing to increase the ΔE_{total}. The ΔE_{hyp} can help to move the r_e from 1.0 Å (ΔE_{Lewis} at Figure 4) to 2.5 Å (Figure 3, panels C and D). In this line, the hyperconjugative

dx.doi.org/10.1021/jp411230w | J. Phys. Chem. A 2014, 118, 5808−5817

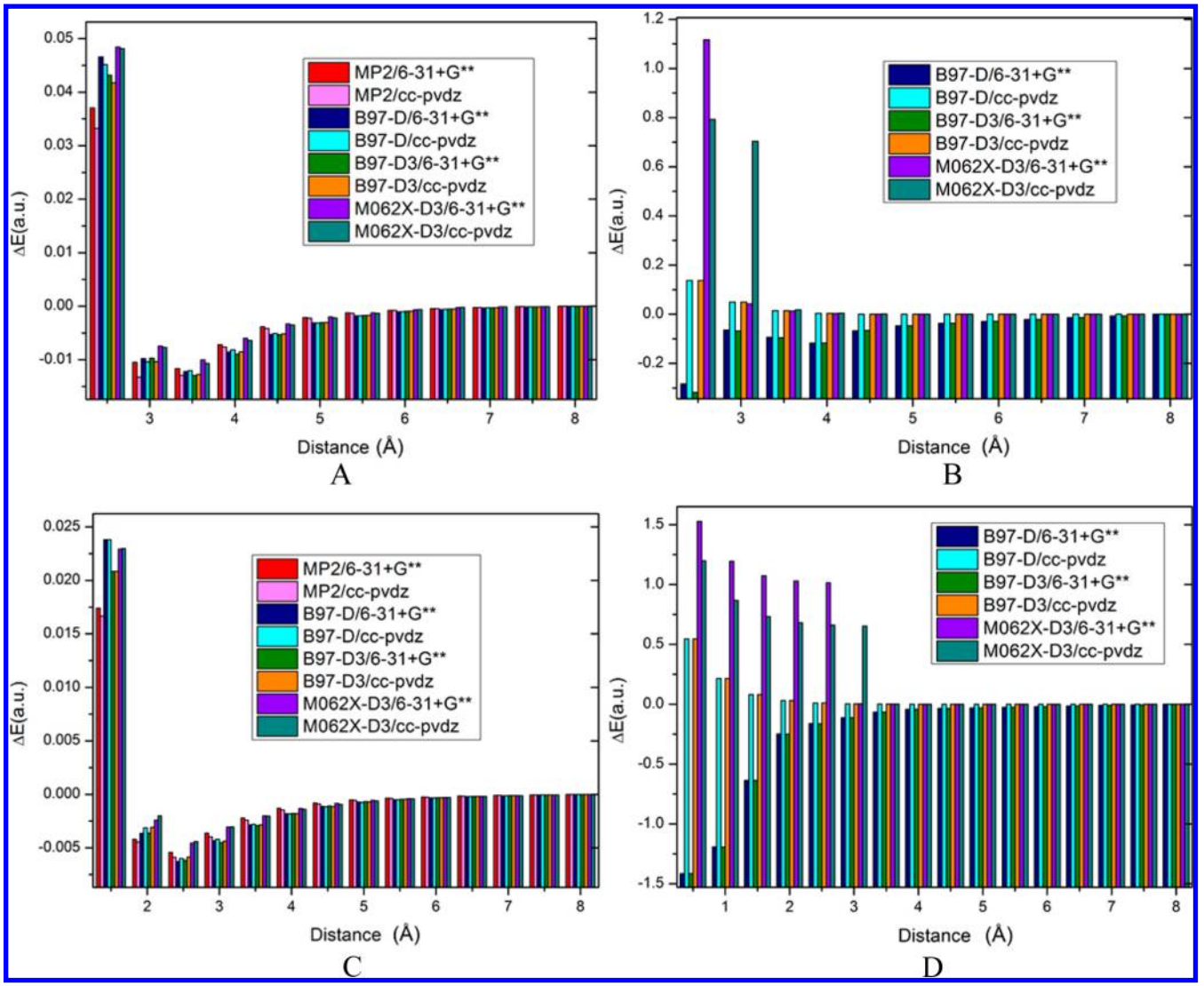

Figure 3. (A) ΔE_{total} and (B) ΔE_{hyp} potential energy curves for parallel eclipsed. (C) ΔE_{total} and (D) ΔE_{hyp} potential energy curves T-shaped.

Table 1. ΔE(re) (a.u.) Comparison with Truncated Values

	MP2		B97-D		B97-D3		M062X-D3	
Conf.	GTO	CBS	GTO	CBS	GTO	CBS	GTO	CBS
PE	−0.0116	−0.0132	−0.0121	−0.0120	−0.0129	−0.0127	−0.0100	−0.0106
PS	−0.0111	−0.0128	−0.0119	−0.0117	−0.0126	−0.0124	−0.0098	−0.0104
PD	−0.0123	−0.0139	−0.0120	−0.0119	−0.0122	−0.0121	−0.0118	−0.0114
Ang	−0.0100	−0.0115	−0.0113	−0.0114	−0.0111	−0.0113	−0.0092	−0.0096
TS	−0.0054	−0.0058	−0.0062	−0.0059	−0.0061	−0.0058	−0.0045	−0.0044

effects can also play a significant role for TS configuration in a hydrophobic environment. Nevertheless, in PE, PS, PD, and Ang, the ΔE_{hyp} will be helpful to stabilize the ΔE_{total}, mainly at lower ranges. For PE and PS, this effect will predominate only at very small distances. The most significant ΔE difference was observed for PD and Ang, 0.5 au and 0.1 au, respectively. For instance, the ΔE_{Lewis} value in Ang is almost 0.25 au at 2.5 Å (Figure 4). The energy decreases dramatically to 0.15 a.u, if ΔE_{hyp} is added. These facts show how the hyperconjugative effects can modulate this interaction, not only for $\pi-\pi^*$ systems. It is well-known that such interaction is due to the sum of steric and hyperconjugative effects, which are in good agreement with our theoretical findings. In fact, the MM technique has a precarious ability to predict those relative energies, mostly those of lower ranged, because of high electronic correlation effects that are involved.

3.2. Reappraisal of Hydrophobic Noncovalent Interactions in Inosine-Phenylalanine: Proposal of an Empirical Correction Term. Until now, our results revealed some care needed for using force fields, specifically dealing with hydrophobic noncovalent interactions. The electronic structure methods displayed some attractive effects, which are not computed by the empirical methods. In line with this, some efforts could be directed to refit the Lennard-Jones (LJ) potential generally incorporated in force fields.

dx.doi.org/10.1021/jp411230w | J. Phys. Chem. A 2014, 118, 5808−5817

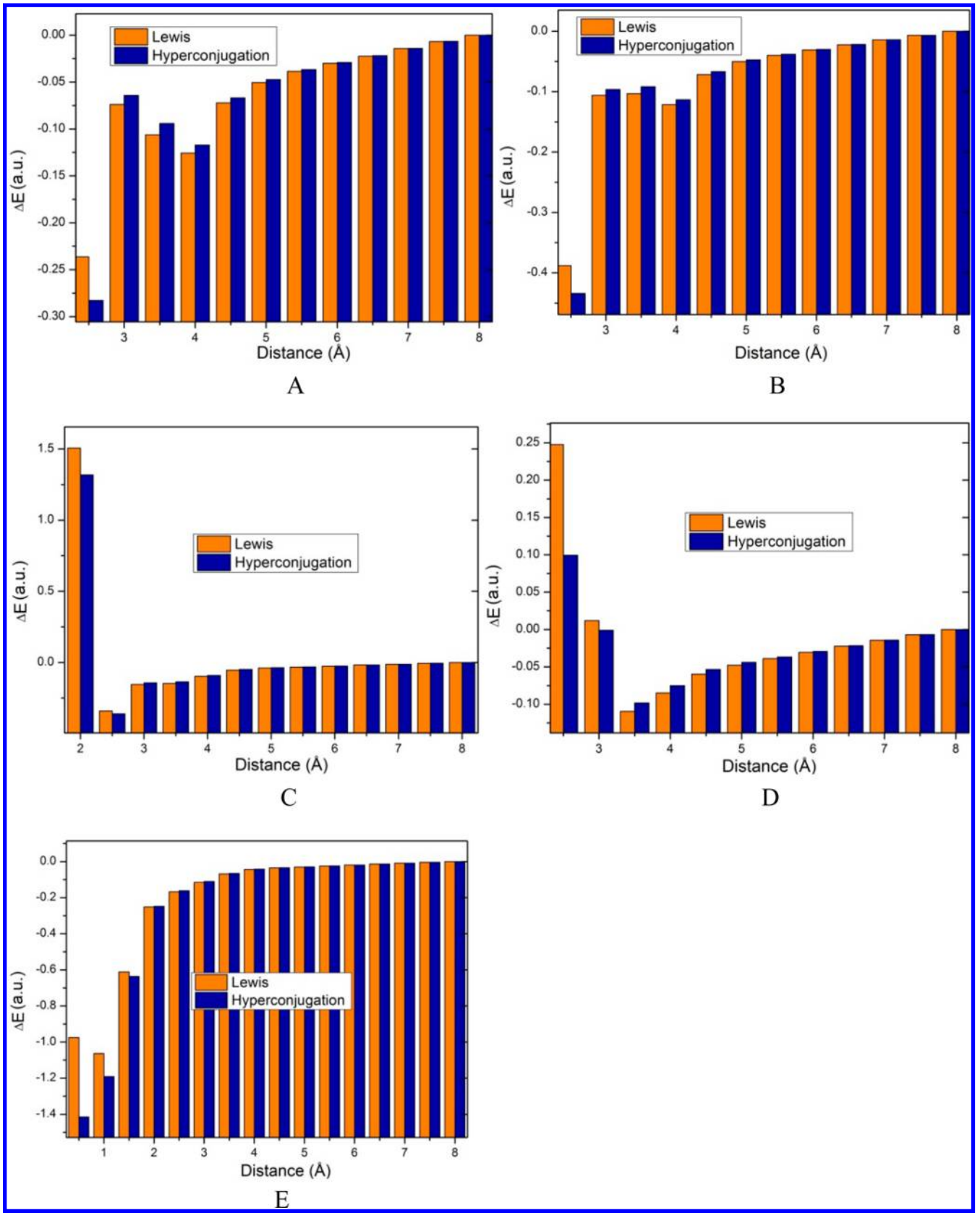

Figure 4. (A) B97-D3/6-31+G**NBOdel calculation results for parallel eclipsed, (B) parallel staggered, (C) parallel displaced, (D) angular, and (E) T-shaped.

The original LJ potential is described by 2. In accordance with our findings, the major flaw of this potential lies in not being able to efficiently predict the repulsion forces and the r_e of some interaction routes. In the LJ potential, the repulsion term is the positive one (eq 5); consequently the negative term is related to attractive forces (eq 6).

dx.doi.org/10.1021/jp411230w | J. Phys. Chem. A 2014, 118, 5808−5817

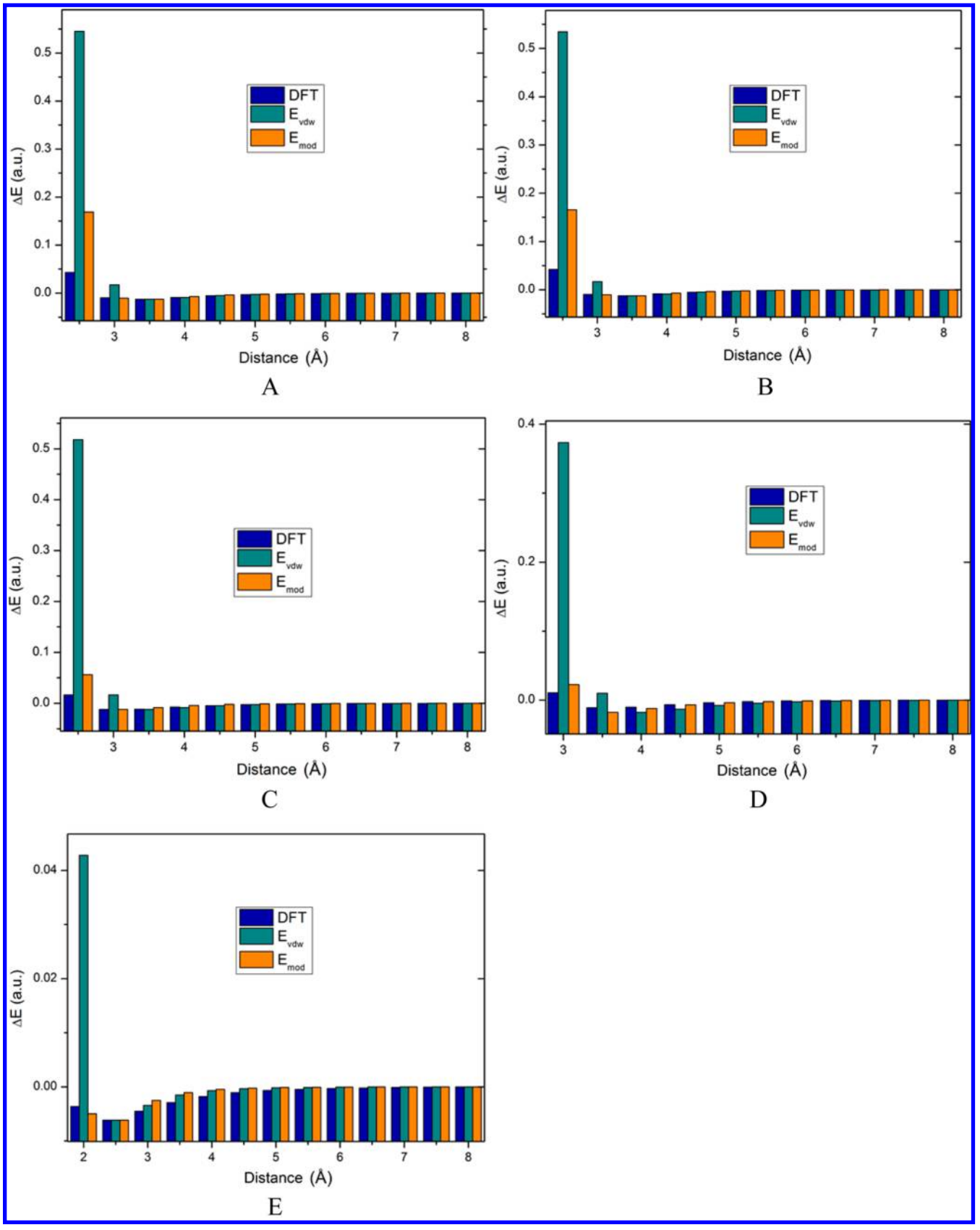

Figure 5. New potential prediction for (A) parallel eclipsed, (B) parallel staggered, (C) parallel displaced, (D) angular, and (E) T-shaped.

$$E_{\mathrm{rep}}(r) = \left(\frac{r_e}{r}\right)^{12} \quad (5)$$

$$E_{\mathrm{att}}(r) = -2\left(\frac{r_e}{r}\right)^{6} \quad (6)$$

dx.doi.org/10.1021/jp411230w | J. Phys. Chem. A 2014, 118, 5808−5817

Table 2. All Parameters for the Potentials in Figure 5, r_e (Å), and ΔE (a.u.)

Conf.	r_e (vdw)	r_e (st)	r_e (DFT)	ΔE_{vdw} (r_e)	ΔE_{st} (r_e)	ΔE_{DFT} (r_e)	δ_{vdw}	δ_{mod}
PE	3.5	3.5	3.5	−0.9860	−1.3187	−0.012 91	0.013 093	0.009790
PS	3.5	3.5	3.5	−0.9860	−1.3187	−0.012 66	0.012 839	0.009600
PD	3.5	3.0	3.0	−0.9860	−2.2090	−0.012 27	0.012 444	0.005555
Ang	4.0	3.5	3.5	−0.9690	−2.2235	−0.011 17	0.018 339	0.007992
TS	2.5	2.5	2.5	−0.9981	−1.6805	−0.006 17	0.006 181	0.003671

Turning to eq 4, our first attempt was to decrease E_{rep}. Since it has a particular value for each case, in our first step, we will assign $\varepsilon = 1$ and discuss this latter. From here, our starting line becomes eq 7 and it will be named E_{st}.

$$E_{st}(r) = \left(\frac{r_e}{r}\right)^{12} - 2\left(\frac{r_e}{r}\right)^{6} \tag{7}$$

To plot a new function able to describe this nature of interaction, we had to compare with B97-D3 potential curves, which were our reference. First of all, we have placed the values of DFT calculations and eq 7 side by side, assuming the E_{DFT} as a reference and the eq 7. If ε is known, it is possible to rewrite a complete modified potential function (E_{mod}). Therefore, to set ε, the following operation has been done (Supporting Information):

$$\varepsilon = \frac{\Delta E_{DFT}(r_e)}{\Delta E_{ST}(r_e)} = \delta \tag{8}$$

Now, we have a new constant, ε, described by eq 8, able to approximate the potential function E_{st} to the B97-D3 method results, which showed to be a satisfactory way to describe this kind of hydrophobic interaction in a similar way to functional B97-D. However, with this new approach, ε loses its old physical meaning and now becomes only a proportionality constant denominated δ.

Our next step is to find a potential function able to predict more accurately r_e through the E_{st} reshuffle. Aware of the LJ potential drawbacks, we tried to modify eq 7, decreasing eq 5. Since the studied conformations have distinct behaviors, the potential was carefully written using two new functions (see the Supporting Information):

$$E_{st}(r) = \left(\frac{r_e}{r + 0,\ 12}\right)^{12} - 2\left(\frac{r_e}{r}\right)^{6} \tag{9}$$

$$E_{st}(r) = \left(\frac{r_e}{1.07r}\right)^{12} - 2\left(\frac{1.0001r_e}{r}\right)^{6} \tag{10}$$

Figure 5 shows a prediction of the new potentials and compares them to the old LJ potential (E_{vdw}). Equation b) was used to plot these curves and 8 to valuate δ in E_{mod} and E_{vdw} 2. Equation) was used to evaluate E_{st} in PE, PS and TS. In PD and Ang, we have used eq 10. All involved parameters for the Phe + Inosine dimer are shown in Table 2.

From Figure 5, it is clear that the repulsive energies were drastically decreased at the proposed potentials. The r_e error was also corrected for PD and Ang. Therefore, we believe these LJ potential rearrangements can improve the force field's ability to predict nonbonded interaction energies for a dimer model that simulates molecular interactions between amino acid residues and nucleoside. Thus, the new potentials proposed in this work are described by eq 11.

$$E_{mod}(r) = \delta\left\{\left(\frac{r_e}{1.07r}\right)^{12} - 2\left(\frac{1.0001r_e}{r}\right)^{6}\right\} \quad \text{or}$$

$$\delta\left\{\left(\frac{r_e}{r + 0.12}\right)^{12} - 2\left(\frac{r_e}{r}\right)^{6}\right\} \tag{11}$$

3.3. MethyltransferaseVP39: A Study Case. In order to illustrate our findings, we have evaluated the hydrophobic noncovalent interactions between methyltransferase VP39 and 3-methylcitosine (PDB code: 3MCT). That is a very important bifunctional vacine protein responsible for mRNA and nucleobases recognition.[47,48] For that protein, it is well-known that the Tyr22 and Phe180 residues provide the major influence in the protein recognition by stacking interactions[14] with the ligand position in the crystallized structure. It can support an interaction with 3-methylcitosine through the two aromatic rings which are localized on the protein perimeter. Thus, the first attempt was to perform a QM/MM calculation evolving the whole protein, confronting those results to UFF calculations. The QM part would be applied only among Tyr22, Phe180, and the ligand. However, the MM region was too large, hiding subtle energy variations. So, theoretical calculations were carried out on the potential energy surface obtained by means of scanning the distance along the X axis (Figure 6) between amino acids residues Tyr22 and Phe180 from the crystal structure (Figure S1 of the Supporting Information) using B97-D3/6-31+G** and UFF methods.

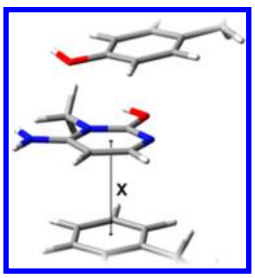

Figure 6. Interaction between 3-methylcitosine and VP39 aromatic residues.

The upper ring (Tyr22) shows a similar position to the angular conformation studied in this work; in contrast, the bottom ring (Phe180) seems to be close to the parallel staggered conformation (Figure 6). By analyzing the interference caused by the presence of two rings, the calculation was executed in three ways: both rings, without the upper ring, and without the bottom ring.

In the crystallized structure, the equilibrium distance is 3.58 Å, matching with DFT calculations; ΔE was obtained from the relation: $\Delta E(r) - \Delta E(r_e)$. So, for correct minima energy values, the potential surface should not have negative energy values and ΔE would always be 0 au. From Figure 7A, we can notice

dx.doi.org/10.1021/jp411230w | J. Phys. Chem. A 2014, 118, 5808−5817

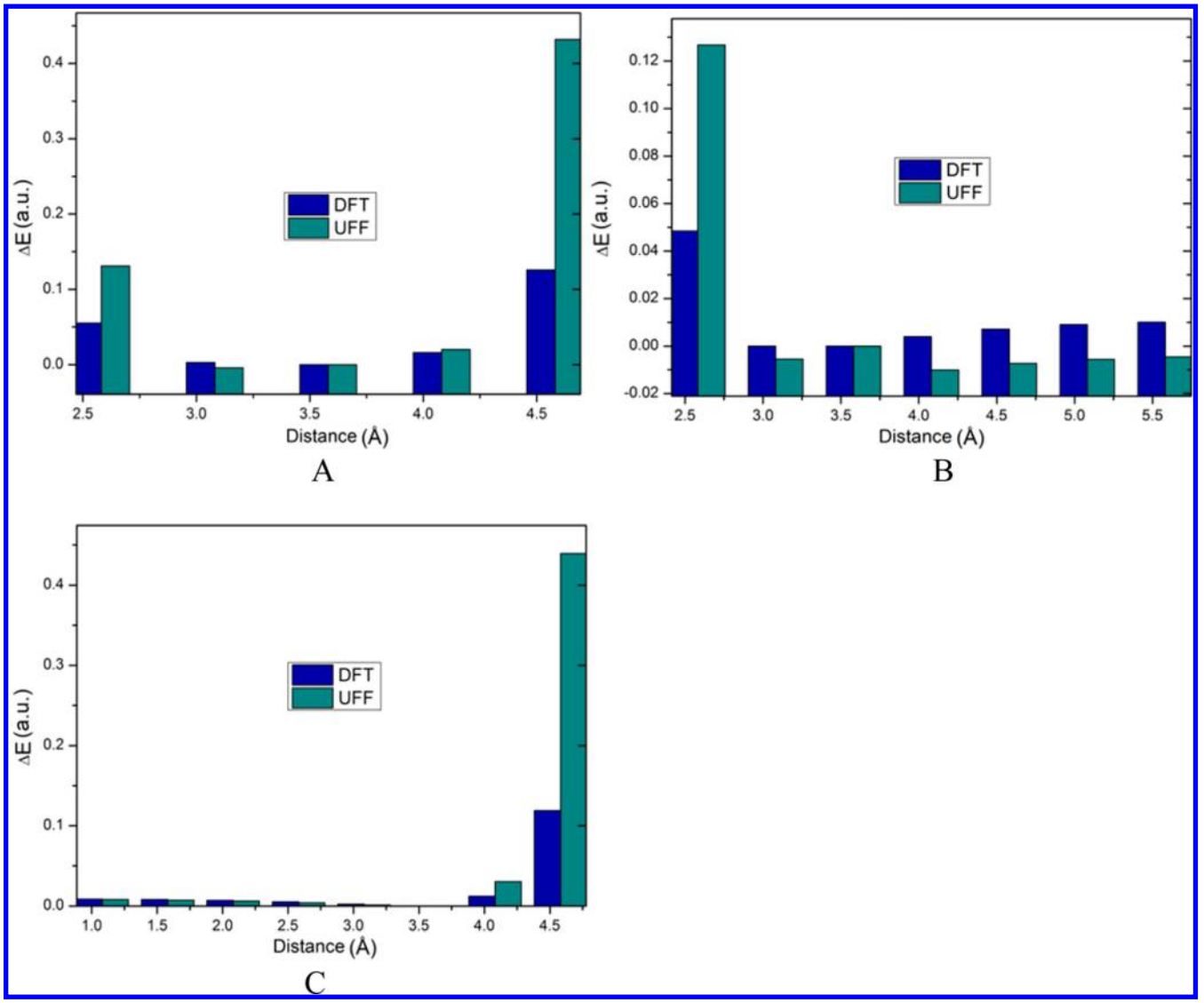

Figure 7. Single point calculations: (A) with both rings, (B) without the upper ring, and (C) without the bottom ring.

that whereas both methods predicted the equilibrium distance well, the UFF results show the same errors considered in previous situations. The repulsive energies at 2.58 and 4.58 Å are so much higher than the DFT results. The same peaks appeared in (B) and (C) due to the ligand interaction with only the bottom ring and only the upper ring, respectively.

In Figure 7B, the UFF data show two minimum points at 3.08 and 4.08 Å with negative energy. All energy values at points after the correct equilibrium distance were also negative. In this case, the universe force field performed the worse result among the three situations. Even showing a good result in (A), it is possible to say that the high values in (C) offset the errors in (B). In this context, eq 11 seems to be useful to circumvent this high values issue. It is well-known that hydrophobic cavities are essential in the molecular recognition process because they can be created in the gas phase or solution, thus generating stable 3D structures for both ligand and receptor. In this context, the development of new empirical potentials from interpolated and analytical PESs could, in principle, be used to take into account the electronic effects, which can play a crucial role in hydrophobic interactions in the molecular recognition process.

4. CONCLUSION

The molecular recognition as well as protein folding are complex problems with many variables. This outlook is still aggravated by the existence of few experimental handles for understanding the individual steps that lead a polypeptide chain to adopt unique and relatively stable three-dimensional conformations appropriate for interaction with another biological molecule. Our results point out that it is a hard task to take into account the hydrophobic interactions, such as $\pi-\pi$ and T-stacking interactions by theoretical calculations using conventional force fields due to quantum effects of hyperconjugation and electronic correlation, which are essential to compute the hydrophobic interactions in proteins.

Actually, our theoretical findings showed that the universal force field is not able to describe interactions among systems with high-electronic correlation because of its implemented nonbonded potential function, the Lennard-Jones potential. Interactions among aromatic rings can be very complex, occurring by a lot of possibilities and may be present either in small molecules or in large compounds, each one with particular effects. In this context, a powerful potential demands to be implemented in the force fields. It could be obtained

dx.doi.org/10.1021/jp411230w | J. Phys. Chem. A 2014, 118, 5808−5817

through simple modifications on the LJ potential, whose errors have been minimized. These potentials may be crucial to the understanding of extensive aromatic systems. Thus, our findings put in evidence that modifications in the Lennard-Jones potential can improve theoretical predictions in scenarios where hydrophobic interactions can drive the molecular recognition.

On the other hand, theoretical calculations using standard force fields could, in some situations, lead to questionable conclusions. Therefore, the development of new empirical potentials from interpolated and analytical PEC can, in principle, be used to take into account the steric and electronic effects. In fact, if appropriate force field methods are used for large systems, in which ab intio calculations are highly computational-demanding, great advances can, in principle, be performed in designing synthetic receptors for nucleobases by optimizing noncovalent host−guest interactions. We feel strongly, then, that those studies might be helpful for exploring protein engineering as well.

■ ASSOCIATED CONTENT

Supporting Information

Quantum versus classical calculations for molecular interaction, hyperconjugation analysis, B97-D3/6-31G+** results, methods and basis set for ΔE_{total} comparison, functional and basis set for ΔE_{Lewis} comparison, functional and basis set for ΔE_{hyp} comparison. This material is available free of charge via the Internet at http://pubs.acs.org.

■ AUTHOR INFORMATION

Corresponding Author

*E-mail: teo@dqi.ufla.br. Fax: 55 35 3829-1271. Tel: 55 35 3829-1522.

Notes

The authors declare no competing financial interest.

■ ACKNOWLEDGMENTS

We thank the Brazilian agencies FAPEMIG, CAPES, and CNPq for funding part of this work. Finally, CNPq and CAPES are also gratefully acknowledged for the fellowships and studentships.

■ REFERENCES

(1) Ben-Naim, A. Strong Forces Between Hydrophilic Macromolecules: Implications in Biological Systems. *J. Chem. Phys.* **1990**, *93*, 8196−8210.
(2) Ramalho, T. C.; da Cunha, E. F. F. Thermodynamic Framework of the Interaction Between Protein and Solvent Drives Protein Folding. *J. Biomol. Struct. Dyn.* **2011**, *28*, 645−646.
(3) Ben-Naim, A. Levinthal's Question Revisited, and Answered. *J. Biomol. Struct. Dyn.* **2012**, *30*, 113−124.
(4) Mittal, A.; Jayaram, B.; Shenoy, S.; Bawa, S. T. A Stoichiometry Driven Universal Spatial Organization of Backbones of Folded Proteins: Are There Chargaff's Rules for Protein Folding? *J. Biomol. Struct. Dyn.* **2010**, *28*, 133−142.
(5) Ramalho, T. C.; Santos, L. A.; da Cunha, E. F. F. Thermodynamic Framework of Hydrophobic/Electrostatic Interactions. *J. Biomol. Struct. Dyn.* **2013**, *31*, 995−1000.
(6) Chandler, D. Interfaces and the Driving Force of Hydrophobic Assembly. *Nature* **2005**, *437*, 640−647.
(7) Vijay, D.; Sakurai, H.; Sastry, G. N. The Impact of Basis Set Superposition Error on the Structure of π-π Dimers. *Int. J. Quantum Chem.* **2011**, *111*, 1893−1901.
(8) Bickelhaupt, M. F. Stacked DNA-Base Quartets: Structure, Chemistry and Computational Intricacies. *Procedia Computer Science* **2010**, *1*, 1147−1148.
(9) Wheeler, S. E. Local Nature of Substituent Effects in Stacking Interactions. *J. Am. Chem. Soc.* **2011**, *133*, 10262−10274.
(10) Reger, D. L.; Debreczeni, A.; Smith, M. D. Rhodium Paddlewheel Dimers Containing the $\pi\cdots\pi$ Stacking, 1,8-Naphthalimide Supramolecular Synthon. *Inorg. Chim. Acta* **2011**, *378*, 42−48.
(11) Yurtsever, E. Pi-Stack Dimers of Small Polyaromatic Hydrocarbons: A Path to the Packing of Graphenes. *J. Phys. Chem. A* **2009**, *113*, 924−930.
(12) Hunter, C. A.; Sanders, J. K. M. The Nature of π-π Interactions. *J. Am. Chem. Soc.* **1990**, *112*, 5525−5534.
(13) Hunter, C. A. Meldola Lecture. The Role of Aromatic Interactions in Molecular Recognition. *Chem. Soc. Rev.* **1994**, *23*, 101−109.
(14) Hu, G.; Gershon, P. D.; Hodel, A. E.; Quiocho, F. A. mRNA Cap Recognition: Dominant Role of Enhanced Stacking Interactions Between Methylated Bases and Protein Aromatic Side Chains. *Proc. Natl. Acad. Sci. U.S.A.* **1999**, *96*, 7149−7154.
(15) Wheeler, S. E.; Houk, K. N. Substituent Effects in the Benzene Dimer Are Due to Direct Interactions of the Substituents with the Unsubstituted Benzene. *J. Am. Chem. Soc.* **2008**, *130*, 10854−10855.
(16) Wheeler, S. E.; McNeil, A. J.; Müller, P.; Swager, T. M.; Houk, K. N. Probing Substituent Effects in Aryl-Aryl Interactions Using Stereoselective Diels-Alder Cycloadditions. *J. Am. Chem. Soc.* **2010**, *132*, 3304−3311.
(17) Josa, D.; Rodríguez-Otero, J.; Cabaleiro-Lago, E. M. A DFT Study of Substituent Effects in Corannulene Dimers. *Phys. Chem. Chem. Phys.* **2011**, *13*, 21139−21145.
(18) Leavens, F. M. V.; Churchill, C. D. M.; Wang, S.; Wetmore, S. D. Evaluating How Discrete Water Molecules Affect Protein-DNA π-π and π^+-π Stacking and T-Shaped Interactions: The Case of Histidine-Adenine Dimers. *J. Phys. Chem. B* **2011**, *115*, 10990−11003.
(19) Wolters, L. P.; Bickelhaupt, F. M. Halogen Bonding Versus Hydrogen Bonding: A Molecular Orbital Perspective. *ChemistryOpen* **2012**, *1*, 96−105.
(20) Josa, D.; Rodríguez-Otero, J.; Cabaleiro-Lago, E. M.; Rellán-Piñeiro, M. Analysis of the Performance of DFT-D, M05-2X and M06-2X Functionals for Studying $\pi\cdots\pi$ Interactions. *Chem. Phys. Lett.* **2013**, *557*, 170−175.
(21) Kuvychko, I. V.; Spisak, S. N.; Chen, Y. S.; Popov, A. A.; Petrukhina, M. A.; Strauss, S. H.; Boltalina, O. V. A Buckybowl with a Lot of Potential: C_5-$C_{20}H_5(CF_3)_5$. *Angew. Chem., Int. Ed.* **2012**, *51*, 4939−4942.
(22) Qiu, Z.; Xia, Y.; Wang, H. MP2 Study on the Stacking Interactions Between 2-Hydroxyadenine and Four DNA Bases. *J. Solution Chem.* **2010**, *39*, 770−777.
(23) Copeland, K. L.; Anderson, J. A.; Farley, A. R.; Cox, J. R.; Tschumper, G. S. Probing Phenylalanine/adenine Pi-Stacking Interactions in Protein Complexes with Explicitly Correlated and CCSD(T) Computations. *J. Phys. Chem. B* **2008**, *112*, 14291−14295.
(24) Patwari, G. N.; Venuvanalingam, P.; Kołaski, M. Phenylacetylene Dimer: Ab Initio and DFT Study. *Chem. Phys.* **2013**, *415*, 150−155.
(25) Karthikeyan, S.; Nagase, S. Origins of the Stability of Imidazole-Imidazole, Benzene-Imidazole, and Benzene-Indole Dimers: CCSD(T)/CBS and SAPT Calculations. *J. Phys. Chem. A* **2012**, *116*, 1694−1700.
(26) Mohamed, M. N. A.; Watts, H. D.; Guo, J.; Catchmark, J. M.; Kubicki, J. D. MP2, Density Functional Theory, and Molecular Mechanical Calculations of C-H$\cdots\pi$ and Hydrogen Bond Interactions in a Cellulose-Binding Module-Cellulose Model System. *Carbohydr. Res.* **2010**, *345*, 1741−1751.
(27) Paier, J.; Marsman, M.; Kresse, G. Why Does the B3LYP Hybrid Functional Fail for Metals? *J. Chem. Phys.* **2007**, *127*, 024103.
(28) Paier, J.; Marsman, M.; Hummer, K.; Kresse, G.; Gerber, I. C.; Angyán, J. G. Screened Hybrid Density Functionals Applied to Solids. *J. Chem. Phys.* **2006**, *124*, 154709.

(29) Ramalho, T. C.; Taft, C. A. Thermal and Solvent Effects on the NMR and UV Parameters of Some Bioreductive Drugs. *J. Chem. Phys.* **2005**, *123*, 054319.
(30) Prytz, Ø.; Flage-Larsen, E. The Influence of Exact Exchange Corrections in van Der Waals Layered Narrow Bandgap Black Phosphorus. *J. Phys. Condens. Matter* **2010**, *22*, 015502.
(31) Huang, Z.; Sun, H. U. I.; Zhang, H.; Wang, Y. U. E.; Li, F. E. I. $\pi-\pi$ Interaction of Quinacridone Derivatives. *J. Comput. Chem.* **2011**, *32*, 2055−2063.
(32) Grimme, S.; Antony, J.; Ehrlich, S.; Krieg, H. A Consistent and Accurate Ab Initio Parametrization of Density Functional Dispersion Correction (DFT-D) for the 94 Elements H-Pu. *J. Chem. Phys.* **2010**, *132*, 154104.
(33) Adesokan, A. A.; Roberts, V. A.; Lee, K. W.; Lins, R. D.; Briggs, J. M. Prediction of HIV-1 Integrase/viral DNA Interactions in the Catalytic Domain by Fast Molecular Docking. *J. Med. Chem.* **2004**, *47*, 821−828.
(34) Neumann, D.; Lehr, C. M.; Lenhof, H. P.; Kohlbacher, O. Computational Modeling of the Sugar-Lectin Interaction. *Adv. Drug Delivery Rev.* **2004**, *56*, 437−457.
(35) Zhao, J.; Roy, S. A.; Nelson, D. J. MD Simulations of Anthrax Edema Factor: Calmodulin Complexes with Mutations in the Edema Factor "Switch a" Region and Docking of 3′-Deoxy ATP into the Adenylyl Cyclase Active Site of Wild-Type and Mutant Edema Factor Variants. *J. Biomol. Struct. Dyn.* **2003**, *21*, 159−170.
(36) Gohlke, H.; Klebe, G. Approaches to the Description and Prediction of the Binding Affinity of Small-Molecule Ligands to Macromolecular Receptors. *Angew. Chem., Int. Ed.* **2002**, *41*, 2644−2676.
(37) Rappé, A. K.; Casewit, C. J.; Colwell, K. S.; Goddard, W. A., III; Skiff, W. M. UFF, A Full Periodic Table Force Field for Molecular Mechanics and Molecular Dynamics Simulations. *J. Am. Chem. Soc.* **1992**, *114*, 10024−10035.
(38) Lennard-Jones, J. E. Cohesion. *Proc. Phys. Soc., London* **1931**, *43*, 461−482.
(39) Wu, X.; Sun, Y.; Li, C.; Yang, W. Parametric Effects of the Potential Energy Function on the Geometrical Features of Ternary Lennard-Jones Clusters. *J. Phys. Chem. A* **2012**, *116*, 8218−8225.
(40) Morse, P. M. Diatomic Molecules According to The Wave Mechanics. II. Vibrational Levels. *Phys. Rev.* **1929**, *34*, 57−64.
(41) Frisch, M. J.; Trucks, G. W.; Schlegel, H. B.; Scuseria, G. E.; Robb, M. A.; Cheeseman, J. R.; Scalmani, G.; Barone, V.; Mennucci, B.; Petersson, G. A.; et al. *Gaussian09*; Gaussian Inc.: Wallingford, CT, 2009.
(42) Shao, Y.; Molnar, L. F.; Jung, Y.; Kussmann, J.; Ochsenfeld, C.; Brown, S. T.; Gilbert, A. T. B.; Slipchenko, L. V.; Levchenko, S. V.; O'Neill, D. P.; et al. *Spartan Pro*; Wavefunction, Inc., 2006.
(43) Glendening, E. D.; Badenhoop, J. K.; Reed, A. E.; Carpenter, J. E.; Bohmann, J. A.; Morales, C. M.; Weinhold, F. *NBO 5.0*; Board of Regents of the University of Wisconsin System: Madison, WI, 2001.
(44) Grimme, S. Semiempirical GGA-Type Density Functional Constructed with a Long-Range Dispersion Correction. *J. Comput. Chem.* **2006**, *26*, 1787−1799.
(45) Wu, X.; Vargas, M. C.; Nayak, S.; Lotrich, V.; Scoles, G. Towards Extending the Applicability of Density Functional Theory to Weakly Bound Systems. *J. Chem. Phys.* **2001**, *115*, 8748−8757.
(46) Denis, P. A. Theoretical Investigation of the Stacking Interactions Between Curved Conjugated Systems and Their Interaction with Fullerenes. *Chem. Phys. Lett.* **2011**, *516*, 82−87.
(47) Gershon, P. D.; Shi, X.; Hodel, A. E. Evidence That the RNA Methylation and poly(A) Polymerase Stimulatory Activities of Vaccinia Virus Protein VP39 Do Not Impinge Upon One Another. *Virology* **1998**, *246*, 253−265.
(48) Shi, X. The Surface Region of the Bifunctional Vaccinia RNA Modifying Protein VP39 That Interfaces with Poly(A) Polymerase Is Remote from the RNA Binding Cleft Used for Its mRNA 5′ Cap Methylation Function. *J. Biol. Chem.* **1997**, *272*, 23292−23302.